Fuzzy Entropy Metrics for the Analysis of Biomedical Signals: Assessment and Comparison

HAMED AZAMI [1], **PENG LI** [2,3], **(Member, IEEE), STEVEN E. ARNOLD** [1],
JAVIER ESCUDERO [4], **(Member, IEEE), AND ANNE HUMEAU-HEURTIER** [5]

[1]Department of Neurology and Massachusetts General Hospital, Harvard Medical School, Charlestown, MA 02129, USA
[2]Division of Sleep and Circadian Disorders, Brigham and Women's Hospital, Harvard Medical School, Boston, MA 02115, USA
[3]School of Control Science and Engineering, Shandong University, Jinan 250061, China
[4]School of Engineering, Institute for Digital Communications, The University of Edinburgh, Edinburgh EH8 9YL, U.K.
[5]LARIS - Laboratoire Angevin de Recherche en Ingénierie des Systèmes, University of Angers, 49035 Angers, France

Corresponding author: Hamed Azami (hazami@mgh.harvard.edu)

ABSTRACT Fuzzy entropy (FuzEn) was introduced to alleviate limitations associated with sample entropy (SampEn) in the analysis of physiological signals. Over the past decade, FuzEn-based methods have been widely used in various real-world biomedical applications. Several fuzzy membership functions (MFs), including triangular, trapezoidal, Z-shaped, bell-shaped, Gaussian, constant-Gaussian, and exponential functions have been employed in FuzEn. However, these FuzEn-based metrics have not been systematically compared yet. Since the threshold value r used in FuzEn is not directly comparable across different MFs, we here propose to apply a defuzzification approach using a surrogate parameter called 'center of gravity' to re-enable a fair and direct comparison. To evaluate these MFs, we analyze several synthetic and three clinical datasets. FuzEn using the triangular, trapezoidal, and Z-shaped MFs may lead to undefined entropy values for short signals, thus providing a very limited advantage over SampEn. When dealing with an equal value of the center of gravity, the Gaussian MF, as the fastest algorithm, results in the highest Hedges' g effect size for long signals. Our results also indicate that the FuzEn based on exponential MF of order four better distinguishes short white, pink, and brown noises, and yields more significant differences for the short real signals based on Hedges' g effect size. The triangular, trapezoidal, and Z-shaped MFs are not recommended for short signals. We propose to use FuzEn with Gaussian and exponential MF of order four for characterization of short (around 50–400 sample points) and long data (longer than 500 sample points), respectively. We expect FuzEn with Gaussian and exponential MF as well as the concept of defuzzification to play prominent roles in the irregularity analysis of biomedical signals. The MATLAB codes for the FuzEn with different MFs are available at https://github.com/HamedAzami/FuzzyEntropy_Matlab.

INDEX TERMS Fuzzy entropy, defuzzification, centre of gravity, fuzzy membership functions, irregularity.

I. INTRODUCTION

Entropy is a powerful and popular nonlinear metric used to assess the dynamical characteristics of time series [1]. Entropy-based approaches have been broadly used in many biomedical applications, such as epilepsy, and Alzheimer's and Parkinson's diseases [2]–[6]. Shannon entropy (ShEn) and conditional entropy (ConEn), which are two common concepts in the analysis of biomedical signals, respectively quantify the amount of information and the rate of information production in signals [1], [3], [7].

The concept of entropy of a fuzzy set was first introduced by De Luca and Termini [8], who defined entropy as a "measure of the degree of fuzziness of a generalized set". This definition of entropy is different from the one of ShEn and ConEn, since no probabilistic concept is required to define it. This function provides a global measure of the "indefiniteness" of the situation of interest. This function can also be considered as the "average intrinsic information" received when one decides to classify ensembles of patterns described by means of fuzzy sets [8]. They also provided a set of

---

The associate editor coordinating the review of this manuscript and approving it for publication was Khalid Aamir.

properties for which the entropy of a fuzzy set should satisfy them. Yager also introduced a measure of entropy that can be used to calculate the amount of uncertainty [9]. Additionally, to deal with both the ShEn and fuzzy sets, Shannon fuzzy entropy was developed [10]. For more information about the combination of ShEn and fuzzy set theory, and its main characteristics and limitations, please see the survey provided by Al-Sharhan *et al*. [11].

However, ShEn-based approaches, unlike ConEn-based ones, are relatively insensitive to signal bandwidth and high-frequency components of a signal [12]. High frequency oscillations of time series are used in many applications; for example, localizing seizure generating regions in epileptic brain [5], [13], [14]. Change in different bands in signals can be used in characterization of some diseases, such as Alzheimer's disease (AD) [6], [15]. Thus, we focus on ConEn-based entropy techniques in this paper.

Sample entropy (SampEn), which is based on ConEn, quantifies the irregularity of signals and it has been widely used in many physiological and non-physiological applications [2], [7], [16]–[19]. SampEn denotes the negative natural logarithm of the conditional probability that two series similar for *m* sample points remain similar at the next sample, where self-matches are not considered in calculating the probability [2].

In the SampEn algorithm, the similarity of embedded vectors is based on the Heaviside function [2]. The Heaviside function can be considered as a conventional two-state classification method. However, in the real-world applications, boundaries between classes may be vague and it is difficult to determine whether an input pattern belongs totally to a class [20]. Furthermore, in spite of its popularity, SampEn leads to either undefined or unreliable results for short signals [4], [21], [22].

To deal with these deficiencies of SampEn, fuzzy entropy (FuzEn) was introduced based on the concept of fuzzy sets and SampEn [23]. It was illustrated that the soft and continuous boundaries of fuzzy functions ensure the continuity. It was found that FuzEn has a stronger relative consistency and less dependence on data length [24]. Accordingly, FuzEn approaches have been used in a wide range of real-world applications ranging from neuroscience and biomedical engineering to mechanical and financial studies [23], [25]–[28].

To assess the similarity of two embedded vectors in SampEn, the distance between these vectors is calculated [2]. However, in the first algorithm of FuzEn [23], the average of each vector (baseline) is first removed from each vector. Then, the differences between these vectors are calculated. In fact, a local trend removal is employed before calculating distances [23]. A balanced quantification of local- and global-similarity was considered in a new definition of FuzEn which is called fuzzy measure entropy (FuzMEn) [29].

Depending on the local and global characteristics of signals, three main FuzEn methods are available [23], [30], [31], but have not been systematically compared.

Moreover, several fuzzy membership functions (MFs) can be used in these algorithms [23], [32], [33].

In this article, we first survey uses of FuzEn drawn from the fields of biomedical engineering. We then detail the advantages and disadvantages of three main forms of FuzEn. The characteristics and limitations of each MF are described as well (e.g., in terms of having smooth shape, being nonzero at all points, and computational time) and their effects on FuzEn are discussed.

A change in parameters used in a fuzzy MF varies its shape, leading to different FuzEn-based results. In addition, there are different numbers and types of parameters for the classical MFs. Accordingly, there is a real need to unify these MFs and establish direct relationships between the parameters used in the MFs. In fact, a direct comparison between the MFS used for FuzEn is not available. Therefore, we propose to use the concept of defuzzification in this article. This allows us to reliably compare the FuzEn with different MFs. The FuzEn metrics with different MFs are compared in terms of sensitivity of the methods to the length of signals, dependency of FuzEn metrics on the periodicity and the degree of randomness in time series, discrimination of short RR interval signals recorded from healthy young vs. elderly subjects, long focal vs. non-focal electroencephalograms (EEGs), and stride interval fluctuations for 3-4 vs 6-7 years old healthy children, and computational time. We finally draw the conclusions and suggest several lines of future research.

II. SURVEY ON BIOMEDICAL APPLICATIONS OF FUZZY ENTROPY METHODS

FuzEn approaches have been used in numerous biomedical applications. Hu studied EEG data for gender recognition [34]. For this purpose, the data were processed with several entropy methods: approximate entropy, SampEn, spectral entropy, and FuzEn. The features given by these entropy measures were then used with six types of classifiers. The results showed that FuzEn and support vector machine give the best results for gender classification – an accuracy of 0.995 and an area under the curve (AUC) of 0.995. Using the Boosting and vote method, classification performances are even better (an accuracy of 0.996 and 0.998, respectively) [34].

FuzEn on EEG data was also used for person authentication [35]. Thus, Mu *et al.* used four types of entropy measures to obtain EEG signal features for person recognition. They revealed that FuzEn achieves the best performance for this task and outperforms the other state-of-the-art methods [35]. Mu *et al.* carried out another study for person authentication [36]. For this purpose, they proposed the stimuli of self-photos and non-self-photos. FuzEn was used to determine and choose the minimum number of EEG electrodes to identify individuals. The results revealed that two electrodes (FP1 and FP2) in the frontal area can lead to interesting results for human recognition [36].

Tibdewal *et al.* studied EEG data – recorded in epileptic and non-epileptic subjects – with Renyi entropy, Shannon

entropy, approximate entropy, SampEn, and FuzEn [37]. They reported that FuzEn outperforms the other entropy measures in terms of discrimination of epileptic from non-epileptic EEG recordings [37]. Xiang *et al.* also studied state inspection of epileptic seizures based on FuzEn [38]. Their results illustrated that FuzEn leads to higher classification accuracy values in comparison with SampEn-based techniques [38].

EEG time series were processed with fuzzy approximate entropy and fuzzy SampEn to detect the abnormality of irregularity and chaotic behavior in the AD brain signals [39]. The results reported by the authors show that fuzzy SampEn leads to higher group differences (AD vs. healthy subjects) in different brain regions and higher average classification accuracy [39]. Fuzzy and SampEn methods were also used for characterization of EEGs in AD [40]. AD patients had significantly lower FuzEn values than control subjects (Student's t-test - $p < 0.01$) at several electrodes. The results illustrated the superiority of FuzEn over SampEn in terms of discrimination of 11 disease patients' from 11 healthy subjects' EEGs [40].

In another study, FuzEn was utilized to monitor EEG recordings during physical exercise [41]. For this purpose, FuzEn was applied to EEG signals during physical exercise workload quantified by the average-to-maximal heart rate ratio (AMHRR). The results illustrated that EEG spectral power and FuzEn show a similar increasing pattern with AMHRR. Nevertheless, FuzEn led to a higher specificity in selecting effective frequency bands (i.e., theta, alpha, and beta) [41]. Other authors used FuzEn and SampEn to characterize and classify EEG sleep stages [42]. The results illustrated that FuzEn leads to better results than SampEn for this task [42].

FuzEn has also been used in a detection system for driver fatigue [43], [44]. Thus, Hu and Wang evaluated sample, fuzzy, approximate, and spectral entropy, to process EEG signals on which noise was added. This led to several feature sets. Classification and ensemble methods were then used to detect driver fatigue. The results showed that the classification accuracy of FuzEn and the combined feature set were better than those obtained with the other feature sets [43]. Another study was carried out in this application as well [44]. A single EEG channel was processed and the results revealed that the best performance is achieved using a combination of channel CP4, FuzEn feature, and the random forest classifier [44].

Monge *et al.* studied the neural dynamics in attention-deficit/hyperactivity disorder (ADHD) [45]. To this end, magnetoencephalographic (MEG) background activity was analyzed with FuzEn. The results obtained reveal that MEG activity is more regular in ADHD patients than in controls. Moreover, statistically significant differences are observed with FuzEn results in the posterior and left temporal regions [45].

FuzEn also led to interesting findings to re-evaluate the relation between surface electromyogram (EMG) and muscle contraction torque in biceps brachii muscles of healthy subjects [46]. Thus, authors computed the root mean square (RMS), SampEn, and FuzEn of EMG data recorded during a series of elbow flexion tasks following different isometric muscle contraction levels. The results obtained with the FuzEn indicated that this measure is able to estimate biceps brachii muscle strength: FuzEn of EMG exhibits an improved linear correlation with the muscle torque compared to the RMS amplitude of EMG [46]. In another study, authors found that FuzEn is a better choice than SampEn to quantify muscle fatigue through the slope of the regression line [29]. Chen *et al.* inspected how approximate, sample, and fuzzy entropy can characterize surface EMG signals for four different motions: hand grasping, hand opening, forearm supination, and forearm pronation. It was found that the FuzEn-based features, compared with those based on sample and approximate entropy, led to the highest classification accuracy [24]. Authors investigated the mechanisms underlying the aging-related changes in the coordination of agonist and antagonist muscles [47]. For this purpose, normalized muscle activation and FuzEn were used to analyze the activities of biceps and triceps. The results showed that FuzEn values for agonist EMG are similar for young and elderly subjects. However, during elbow extension, FuzEn of antagonist EMG is significantly higher for the elderly group [47].

FuzEn was employed for automated detection of coronary artery disease using electrocardiogram (ECG) signals [48]. The results showed that the FuzEn of coronary artery disease ECGs is higher than that of controls' recordings. This fact may be associated with reduced heart pump function [48].

FuzEn was also used in the domain of prediction of defibrillation success. Thus, by analyzing ECG during ventricular fibrillation, authors used, adapted, and characterized six entropy indices for ventricular fibrillation shock outcome prediction [49]. The performance of the entropy measures was characterized regarding the embedding dimension m and matching tolerance or threshold r. Six classical predictors were also evaluated as baseline prediction values. The best predictions were given by FuzEn [49].

FuzEn has led to some interesting findings in speech signal endpoint detection under low signal-to-noise ratio (SNR) circumstance [50], [51]. Thus, Zhang and Ni proposed a voice activity detection algorithm based on FuzEn and improved relevance vector machine [50]. The results showed good performances in detecting speech under various noisy environments [50]. Another study used FuzEn for voice activity detection [51]. Thus, Elton *et al.* utilized the FuzEn measure as a feature extracted from noise-reduced speech signals to train a support vector machine model for speech/non-speech classification. The results illustrated that the proposed method is more efficient than previous standardized voice activity detection algorithms as well as recently developed methods in detecting speech under various noisy environments [51].

TABLE 1. Ability to compute FuzEn with $m = 1$, consideration of the local and global characteristics of embedded vectors, and computational time for FuzEn$^{(Glb)}$, FuzEn$^{(Loc)}$, and FuzMEn in comparison with the popular SampEn.

Characteristics	FuzEn$^{(Glb)}$	FuzEn$^{(Loc)}$	FuzMEn	SampEn
Able to compute FuzEn with $m = 1$	Yes	No	No	Yes
Consideration of global characteristics	Yes	No	Yes	Yes
Consideration of local characteristics	No	Yes	Yes	No
Computational time	Close to SampEn	Close to SampEn	Two times higher than FuzEn$^{(Glb)}$	Close to FuzEn$^{(Glb)}$

The fuzzy measure entropy (a variant of the FuzEn that uses the fuzzy local and fuzzy global measure entropy) was used to analyze heart rate variability (HRV) signals recorded from healthy subjects and patients suffering from heart failure [30]. It has proved to give good results for clinical HRV applications [30].

FuzEn with constant-Gaussian MF was proposed by Ji *et al.* [52]. The new measure was utilized to evaluate clinical short-term (5 min) HRV and cardiac diastolic period variability (DPV) of the patients with coronary artery stenosis and healthy volunteers. The results showed that the new measure applied to clinical DPV outperforms SampEn and FuzEn in distinguishing the patient group and the healthy group [52].

III. REVIEW OF FUZZY ENTROPY METHODS

This Section first details three FuzEn methods based on the local and global characteristics of signals. How to choose the parameters of these approaches is next described.

A. FUZZY ENTROPY METHODS

Assume a univariate time series of length N: $x = \{x_1, x_2, \ldots, x_j, \ldots, x_N\}$. All the template vectors $x_\Lambda^{m,d}$ ($\Lambda = 1, 2, \ldots, N - (m-1)d$) are first created as follows:

$$x_\Lambda^{m,d} = \{x_\Lambda, x_{\Lambda+d}, \ldots, x_{\Lambda+(m-1)d}\}, \quad (1)$$

where m and d respectively denote the embedding dimension and time delay. Next, the distance between each of $x_\Lambda^{m,d}$ and $x_\lambda^{m,d}$ is defined as $\Delta_{\Lambda,\lambda}^{(Loc)} = ChebDist[x_\Lambda^{m,d} - x0(\Lambda), x_\lambda^{m,d} - x0(\lambda)]$, $\Lambda \neq \lambda$, where $x0(\Lambda)$ is the average of $\{x_\Lambda, x_{\Lambda+d}, \ldots, x_{\Lambda+(m-1)d}\}$ to remove the baseline [23]. Loc denotes the local characteristics of embedded vectors.

This algorithm of FuzEn deals with the local characteristics of the sequence, without considering their global characteristics [30]. This is in contrast with the SampEn algorithm, which does consider the global characteristics of the signals. For example, assume $x_\Lambda^{3,1} = \{1, 0.5, 1.5\}$, $x_\lambda^{3,1} = \{3, 2.5, 3.5\}$, and SD of x is equal to 1. Thus, $\Delta_{\Lambda,\lambda}^{(Loc)}$ is equal to 0, although $x_\Lambda^{3,1}$ and $x_\lambda^{3,1}$ are far from each other. This is, in fact, in contradiction with the approach of SampEn [2].

Therefore, we decide to take into account only the global average of the signal ($\bar{x}$). As $\Delta_{\Lambda,\lambda}^{(Glb)} = ChebDist[x_\Lambda^{m,d} - \bar{x}, x_\lambda^{m,d} - \bar{x}] = ChebDist[x_\Lambda^{m,d}, x_\lambda^{m,d}]$, we do not need to consider the global average as well.

Given a FuzEn power n_e and threshold r, the similarity degree is calculated through the exponential MF

$\theta(\Delta_{\Lambda,\lambda}, r) = \exp\left(-\frac{\Delta_{\Lambda,\lambda}^{n_e}}{r}\right)$. Of note is that several well-known fuzzy MFs are described in Subsection III-D.

The function $\psi^{m,d}(n_e, r)$ is then calculated as follows [23]:

$$\psi^{m,d}(n_e, r)$$
$$= \frac{1}{(N-md)(N-md-1)} \sum_{\Lambda=1}^{N-md} \sum_{\lambda=1,\lambda\neq\Lambda}^{N-md} \exp\left(-\frac{\Delta_{\Lambda,\lambda}^{n_e}}{r}\right). \quad (2)$$

Finally, the FuzEn of the signal is defined as the negative natural logarithm of the ratio of $\psi^{m,d}(n_e, r)$ and $\psi^{m+1,d}(n_e, r)$ (computed following the same procedure for the embedding dimension $m + 1$) [23]:

$$\text{FuzEn}(x, m, r, n_e, d) = -\ln\left(\frac{\psi^{m+1,d}(n_e, r)}{\psi^{m,d}(n_e, r)}\right). \quad (3)$$

As mentioned before, this algorithm of FuzEn focuses only on the local characteristics of the embedded vectors of time series. In fact, no global fluctuation is taken into account [30]. This is why the FuzMEn was introduced in 2013 by Liu *et al.*: the fuzzy measure entropy integrates both local and global characteristics and can reflect the entire irregularity in a signal [30]. It has been reported that fuzzy measure entropy has better discrimination ability than FuzEn [30]. To overcome the same problem, Zhu *et al.* proposed FuzEn based on the global characteristics of the embedded vectors of a signal (FuzEn$^{(Glb)}$) [53].

A shortcoming of FuzMEn and FuzEn$^{(Loc)}$ is that the embedding dimension m should be larger than 1. Otherwise, $\Delta_{\Lambda,\lambda}^{(Loc)}$ is always equal to 0. This is particularly relevant when working with short signals. To sum up, the characteristics and limitations of FuzEn$^{(Glb)}$, FuzEn$^{(Loc)}$, FuzMEn, and SampEn are explained in Table 1. In this article, we consider FuzEn$^{(Glb)}$ as the direct extension of SampEn.

B. FUZZY ENTROPY-BASED COMPLEXITY METHODS

The algorithm of MFE includes the following two steps:

1) Univariate coarse-graining process: Assume we have a univariate signal of length L: $u = \{u_1, u_2, \ldots, u_i, \ldots, u_L\}$. In the coarse-graining process, the original signal u is first divided into non-overlapping segments of length τ, named scale factor. Then, the average of each segment is calculated

to derive the coarse-grained signals as follows [54]:

$$x_j^{(\tau)} = \frac{1}{\tau} \sum_{i=(j-1)\tau+1}^{j\tau} u_i, \quad 1 \le j \le \left\lfloor \frac{L}{\tau} \right\rfloor = N. \quad (4)$$

2) Calculation of FuzEn: The FuzEn value is calculated for each coarse-grained signal $x^{(\tau)} = \{x_j^{(\tau)}\}$.

C. PARAMETERS OF FUZZY ENTROPY METHODS

There are three main parameters for the FuzEn methods, including the embedding dimension m, threshold r (or equivalently, Cr, as in our formulation below), and time delay d. It is advisable to use $d > 1$ for oversampled signals. However, some information regarding the frequency of time series may be ignored and the phenomenon of aliasing may also occur for $d > 1$ [4]. Thus, like previous studies about entropy methods [2], [23], d is set to 1 for simplicity.

The embedding dimension m is the length of sequences to be compared. Larger m allows more detailed reconstruction of the dynamic process, while a large value of m is unfavorable because of the need of a very large number of sample points ($10^m - 20^m$), which is hard to meet for physiological or even non-physiological data [2], [23].

The parameter r is chosen to balance the quality of logarithmic likelihood estimates with the loss of signal information. When r is too small, poor conditional probability estimates are achieved. Furthermore, to avoid the effect of noise on data, larger r is recommended. In contrast, for a large r value, too much detailed data information is lost. Therefore, a trade-off between large and small r values is needed [2], [23]. Lake *et al.* proposed an approach to optimally select r [55]. However, since it is needed to calculate SampEn for a range of r and then pick the value that leads to best performance of FuzEn, this may be too time-consuming [56]. To alleviate this problem, a method based on the heuristic stochastic model was proposed to automatically determine r [56]. However, this approach still considers a number of r values leading to computational burden.

For SampEn, it is quite common to set the threshold r as a constant (usually 0.2) multiplied by the standard deviation (SD) of the original signal [2], [23], [54]. This strategy makes SampEn a scale-invariant measure [2], [55]. However, its equivalent values for FuzEn with different fuzzy MFs have not been studied yet. Furthermore, a change in parameters used in a fuzzy MF varies its shape, leading to different FuzEn-based results. Moreover, there exist different numbers and kinds of parameters for the classical MFs. Therefore, it is required to unify these MFs and establish direct relationships between these parameters. To this end, we use the concept of "defuzzification."

A defuzzification process maps a fuzzy set and its corresponding membership degrees into a quantifiable value [57]. In fact, defuzzification is the inverse process of fuzzification [58]. There are a number of defuzzification approaches [57], [59]. In this paper, we use the centroid technique (also called centre of area or gravity), as the most prevalent and physically appealing of all the defuzzification approaches [59], [60]. The centre of gravity for the fuzzy set $\theta(\Delta_{\Lambda,\lambda}, r)$ is calculated as follows [59]:

$$Cr(\theta(\Delta_{\Lambda,\lambda}, r)) = \frac{\sum_{\Delta_{\Lambda,\lambda}} \Delta_{\Lambda,\lambda} \theta(\Delta_{\Lambda,\lambda}, r)}{\sum_{\Delta_{\Lambda,\lambda}} \theta(\Delta_{\Lambda,\lambda}, r)}, \quad (5)$$

where the centroid Cr is a function of the threshold r.

D. FUZZY MEMBERSHIP FUNCTIONS

Different types of fuzzy MFs are shown in Fig. 1. The definition, centre of gravity, and advantages and disadvantages of each of them are discussed in this Subsection. To compare the fuzzy MFs, we consider different centroids ($Cr = 0.05, 0.1, 0.15, 0.2,$ and 0.25). The results are shown in Fig. 2.

As mentioned before, finding the optimum value of Cr (or equivalently r) is time-consuming. Since $r = 0.2$ for SampEn corresponds to $Cr = 0.1$, herein, we set $Cr = 0.1$ for all the FuzEn-based simulations below to fairly compare these techniques.

1) TRIANGULAR MEMBERSHIP FUNCTION

As a piecewise linear, triangular function is one of the simplest fuzzy MFs [61], [62]. This fuzzy MF is defined as follows:

$$\theta(\Delta_{\Lambda,\lambda}, r) = \begin{cases} 1 - \dfrac{\Delta_{\Lambda,\lambda}}{r}, & \Delta_{\Lambda,\lambda} \le r \\ 0, & \Delta_{\Lambda,\lambda} > r \end{cases} \quad (6)$$

The centroid of this fuzzy MF is calculated based on Equation (5) as follows:

$$Cr = \frac{r}{3}. \quad (7)$$

However, FuzEn based on triangular MF may lead to undefined results for short signals (please see Fig. 3) because it is possible for the count $\psi^{m,d}(n_e, r)$ in Equation 3 to have a value of exactly 0.

2) TRAPEZOIDAL MEMBERSHIP FUNCTION

As another piecewise linear function, the trapezoidal MF and its corresponding centroid are respectively computed as [61], [63]:

$$\theta(\Delta_{\Lambda,\lambda}, r) = \begin{cases} 1, & \Delta_{\Lambda,\lambda} \le r \\ \dfrac{-\Delta_{\Lambda,\lambda}}{r} + 2, & r \le \Delta_{\Lambda,\lambda} \le 2r \\ 0, & \Delta_{\Lambda,\lambda} > 2r \end{cases} \quad (8)$$

and

$$Cr = \frac{7}{9}r. \quad (9)$$

Due to their simple formulas and low computational time, both the triangular and trapezoidal MFs have been used extensively, especially in real-time applications [64]. Nevertheless, as these MFs are composed of straight line segments, they are not smooth at the corner points.
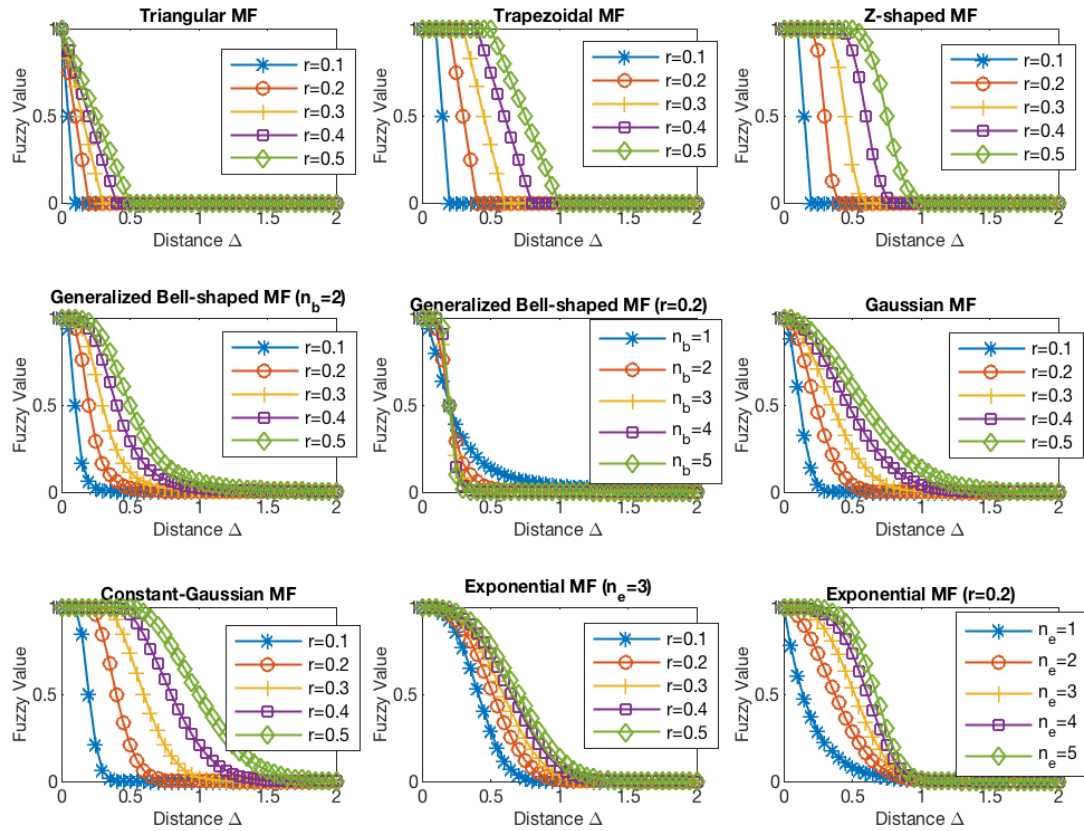
FIGURE 1. Different types of fuzzy membership functions with different *r* values.

3) Z-SHAPED MEMBERSHIP FUNCTION

As a spline-based function, the Z-shaped MF is calculated as follows [32]:

$$
\theta(\Delta_{\Lambda,\lambda}, r) = \begin{cases} 1, & \Delta_{\Lambda,\lambda} \leq r \\ 1 - 2\left(\dfrac{\Delta_{\Lambda,\lambda} - r}{r}\right)^2, & r \leq \Delta_{\Lambda,\lambda} \leq \frac{3}{2}r \\ 2\left(\dfrac{\Delta_{\Lambda,\lambda} - 2r}{r}\right)^2, & \frac{3}{2}r \leq \Delta_{\Lambda,\lambda} \leq 2r \\ 0, & \Delta_{\Lambda,\lambda} > 2r \end{cases}
$$
(10)

The relationship between the centroid *Cr* and threshold *r* for the Z-shaped MF is calculated as:

$$
Cr = \frac{55}{72}r.
$$
(11)

This MF is not smooth at the corner points as well. In the following, we introduce other types of MFs defined by smooth and nonlinear functions.

4) GENERALIZED BELL-SHAPED MEMBERSHIP FUNCTION

Because of their smoothness, nonzero at all points and concise notation, bell-shaped, Gaussian, and exponential MFs are becoming increasingly popular for specifying fuzzy sets [65], [66]. The generalized bell-shaped MF (also called

Cauchy MF) is a direct generalization of the Cauchy distribution used in probability theory [64]. The bell-shaped function is defined as follows [67]:

$$
\theta(\Delta_{\Lambda,\lambda}, r, n_b) = \frac{1}{1 + \left|\dfrac{\Delta_{\Lambda,\lambda}}{r}\right|^{2n_b}},
$$
(12)

where n_b is the fuzzy power of the generalized bell-shaped function. The relationship between the centroid *Cr* and threshold *r* is illustrated as follows:

$$
Cr = r\frac{\sin(\frac{\pi}{2n_b})}{\sin(\frac{\pi}{n_b})}.
$$
(13)

5) GAUSSIAN MEMBERSHIP FUNCTION

The Gaussian MF is defined as follows [32], [63]:

$$
\theta(\Delta_{\Lambda,\lambda}, r) = \exp\left(-\frac{\Delta_{\Lambda,\lambda}^2}{2r^2}\right).
$$
(14)

The centroid *Cr* of this fuzzy MF is calculated as:

$$
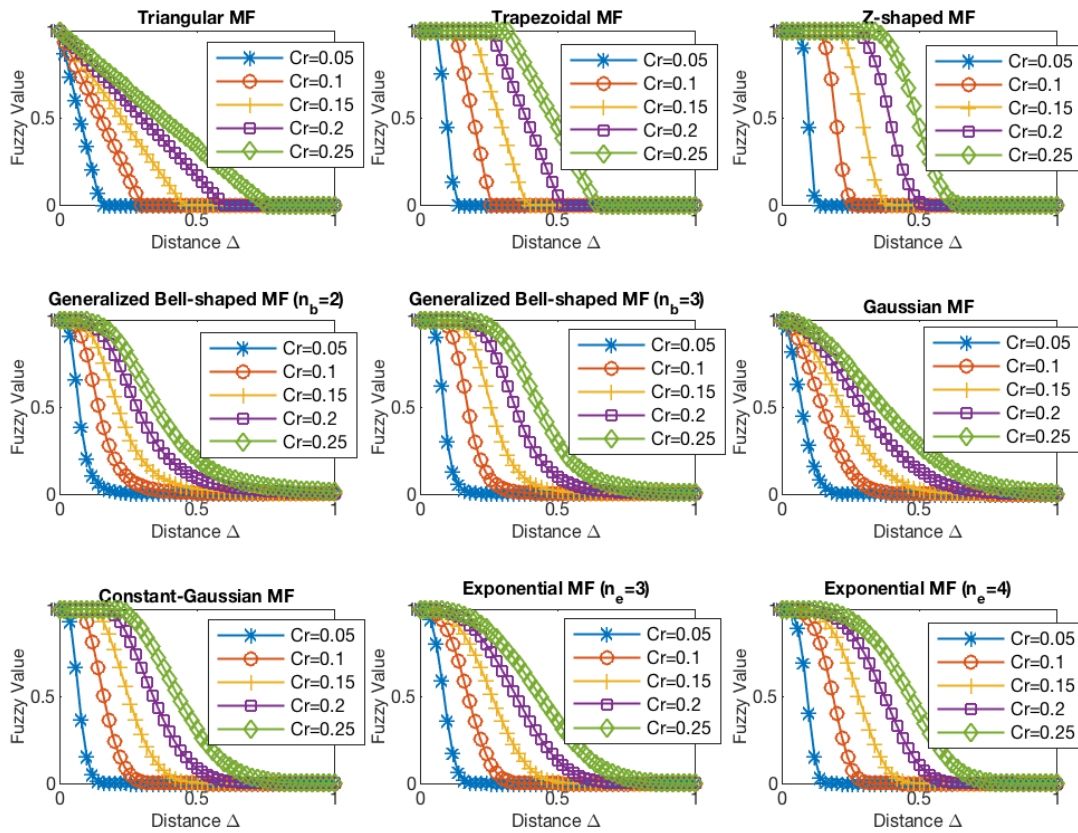Cr = r\sqrt{\frac{2}{\pi}}.
$$
(15)

FIGURE 2. Different types of fuzzy membership functions with different *Cr* values.

6) CONSTANT-GAUSSIAN MEMBERSHIP FUNCTION
The constant-Gaussian MF is defined as follows [33]:

$$\theta(\Delta_{\Lambda,\lambda}, r) = \begin{cases} 1, & \Delta_{\Lambda,\lambda} \leq r \\ \exp\left(-\ln(2)\left(\frac{r - \Delta_{\Lambda,\lambda}}{r}\right)^2\right), & \Delta_{\Lambda,\lambda} > r \end{cases}$$
(16)

Based on Equation (5), the centroid of this function is calculated as:

$$Cr = \frac{0.5 + \frac{0.5}{\ln(2)} + \sqrt{\frac{\pi}{4\ln(2)}}}{1 + \sqrt{\frac{\pi}{4\ln(2)}}} r.$$
(17)

7) EXPONENTIAL MEMBERSHIP FUNCTION
The exponential MF, as the generalized case of Gaussian MF, is defined as follows [23]:

$$\theta(\Delta_{\Lambda,\lambda}, r, n_e) = \exp\left(-\frac{\Delta_{\Lambda,\lambda}^{n_e}}{r}\right),$$
(18)

where n_e denotes the fuzzy power of the exponential MF. When $n_e = 2$, the exponential is equal to the Gaussian MF. Therefore, we set $n_e = 3$ and 4 in the simulations below.

The relationship between the centroid Cr and threshold r for the exponential MF is calculated as:

$$Cr = r^{\frac{1}{n}} \frac{\Gamma(\frac{2}{n_e})}{\Gamma(\frac{1}{n_e})},$$
(19)

where Γ denotes the gamma function.

IV. SIGNALS FOR COMPARISON OF FUZZY ENTROPY METRICS
In this Section, we introduce the synthetic and real signals used to investigate the behavior of entropy approaches.

A. SYNTHETIC SIGNALS
1) FUZZY ENTROPY METHODS VS. NOISE SIGNALS
White, pink, and brown noises are three well-known noise [68], [69]. White noise is a random signal which has an equal energy across all frequencies. The power spectral density of white noise is as $S(f) = C_w$, where C_w is a constant [69]. Pink and brown noise are random processes appropriate for modeling evolutionary or developmental systems [70]. The power spectral density $S(f)$ of pink and brown noise are as $\frac{C_p}{f}$ and $\frac{C_b}{f^2}$, respectively, where C_p and C_b are constants [69], [70].

2) FUZZY ENTROPY METHODS VS. CHANGES FROM PERIODICITY TO RANDOMNESS

A wide range of real signals, especially those created by biological systems, most likely include deterministic and stochastic components [54]. Hence, to inspect how entropy methods change when a stochastic sequence turns into a periodic deterministic signal, we generated a MIX process [71], [72]. It is defined as follows:

$$\text{MIX}_j = (1 - z_j)x_j + z_j y_j, \quad 1 \le j \le N, \quad (20)$$

where N is the length of the signal vectors $z = \{z_j\}$, $MIX = \{MIX_j\}$, and $y = \{y_j\}$. z denotes a random variable which equals 1 with probability p and equals 0 with probability $1 - p$. x shows a periodic time series created by $x_j = \sqrt{2} \sin(2\pi j/12)$, and y is a uniformly distributed series on $\left[-\sqrt{3}, \sqrt{3}\right]$ [72].

B. REAL DATASETS

Entropy-based approaches are widely employed to characterize physiological signals, such as EEG, ECG, and blood pressure recordings [4], [71], [73]. To this end, two non-invasive EEG [74] and ECG datasets [75] are used in this article to distinguish different kinds of dynamics of signals.

1) DATASET OF FOCAL AND NON-FOCAL BRAIN ACTIVITY

The ability of FuzEn techniques to discriminate focal from non-focal signals is evaluated by the use of an EEG dataset (publicly-available at http://ntsa.upf.edu/) [74]. The dataset includes 5 patients and, for each patient, there are 750 focal and 750 non-focal bivariate time series. The length of each signal was 20 s with sampling frequency of 512 Hz (10240 samples). For more information, please refer to [74]. All subjects gave written informed consent that their signals from long-term EEG might be used for research purposes [74]. Before computing the entropies, the time series were digitally filtered using a Hamming window FIR band-pass filter of order 200 and cut-off frequencies 0.5 Hz and 40 Hz, a band typically used in the analysis of brain activity.

2) RR INTERVAL DATA: HEALTHY YOUNG VS. HEALTHY ELDERLY SUBJECTS

We used data from Fantasia database which is publicly-available on PhysioNet website (www.physionet.org) [75]. The database consists of 20 young (21-34 years old) and 20 old (68-85 years old) healthy subjects with their health status having been confirmed rigorously. ECG recordings were continuously collected for 120 min in supine position at a sampling frequency of 250 Hz while the subjects were watching the movie Fantasia to help maintain wakefulness [76]. R-peaks in ECGs were extracted from the beat annotation files that are incorporated in the database. Consecutive normal sinus R-R intervals formed RR interval time series.

3) GAIT MATURATION DATABASE

We also applied the FuzEn methods to the gait maturation database to distinguish the effect of age on the intrinsic stride-to-stride dynamics [77]. The dataset is available at www.physionet.org. A subset including 31 healthy boys and girls is considered in this study in which there were similar numbers of boys and girls in each age group. The children were classified into two age groups: 3 and 4 years old (11 subjects) and 6 and 7 years old children (20 subjects). Height and weight of the young and elderly groups were 105 ± 2 cm and 125 ± 1 cm, and 17.3 ± 0.7 kg, and 25.3 ± 0.9 kg, respectively. The time series recorded from the subjects walking at their normal pace have the lengths of about 400–500 sample points. For more information, please see [77].

V. RESULTS AND DISCUSSION

A. SYNTHETIC SIGNALS

1) FUZZY ENTROPY METHODS VS. NOISE SIGNALS

To assess the sensitivity of FuzEn with different MFs to the time series length, we use 40 realizations of white, pink, and brown noises. The signal length changes from 10 to 1,000 sample points. The profiles, depicted in Fig. 3, suggest that the greater the number of sample points, the more robust the entropy estimates, as seen from the errorbars, which represent the SD.
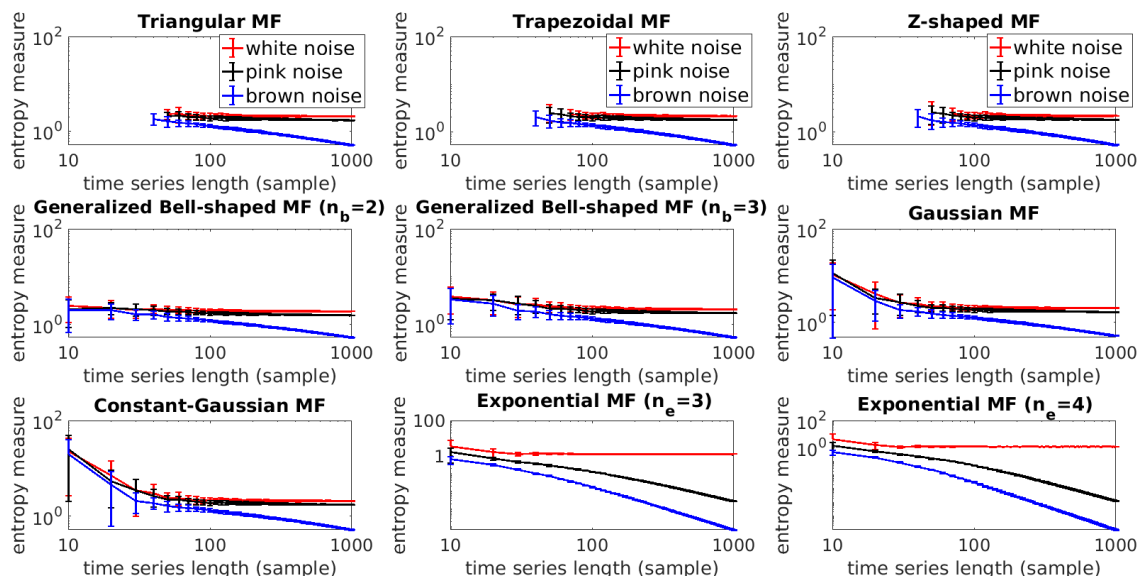
In the FuzEn method with triangular, trapezoidal, and Z-shaped MFs, those differences that are smaller than or equal to r (for triangular MF) or $2r$ (for trapezoidal and Z-shaped MFs) are considered. When the time series length is too small, no differences may be considered, leading to undefined values. This fact is shown in Fig. 3. Thus, we use the other four fuzzy MFs in all the simulations below. Among these for FuzEn metrics, as can be seen in Fig. 3, FuzEn with exponential MF better distinguishes short white, pink, and black noise.

#### 2) FUZZY ENTROPY METHODS VS. CHANGES FROM PERIODICITY TO RANDOMNESS

The FuzEn approaches are applied to 40 realizations of the MIX process with lengths 100 and 1,000 sample points and $p = 0, 0.1, 0.2, 0.3, 0.4, 0.5, 0.6, 0.7, 0.8, 0.9$, and 1. The mean and SD values of the results are depicted in Fig. 4. The profiles show an increase in the irregularity of signals with an increase in the value of p for the MIX process. It is in agreement with the fact that the higher the value of p for a MIX process, the more irregular the time series [71], [72].

To compare the results obtained by FuzEn with different fuzzy MFs, we utilized the coefficient of variation (CV) defined as the SD divided by the mean. We use such a metric as the SDs of time series may increase or decrease proportionally to the mean. The sum of CV values for the MIX process with length 100 and 1,000 sample points are illustrated in Table 2. It is found that the larger the length of signals, the more stable the results. The smallest CVs for short (100 samples) and long signals (1,000 samples) are

FIGURE 3. Mean and SD of results obtained by FuzEn with different MFs for 40 realizations of white, pink, and brown noises. The entropy values obtained by FuzEn with triangular, trapezoidal, and Z-shaped MFs are undefined for short noise signals. Logarithm scale for both the axis is used.
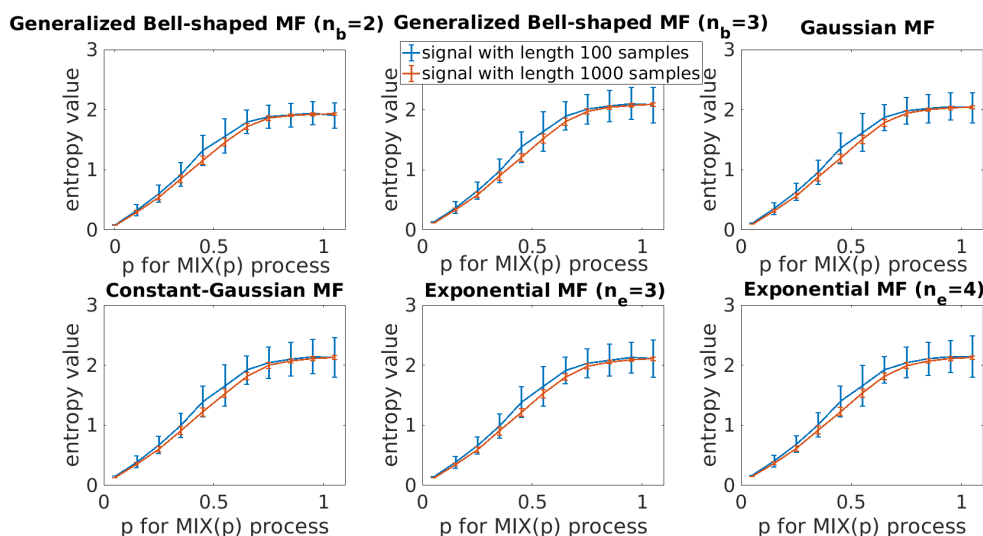
FIGURE 4. Mean and SD of results obtained by FuzEn with different types of fuzzy MFs for MIX(*p*) (0 ≤ *p* ≤ 1).

obtained by FuzEn with generalized bell-shaped ($n_b = 2$) and exponential ($n_e = 4$) MF, respectively. Nevertheless, there is not a big difference between the techniques.

B. REAL DATASETS

### 1) DATASET OF FOCAL AND NON-FOCAL BRAIN ACTIVITY

For the focal and non-focal EEG recordings, the mean and median of results obtained by FuzEn with different MFs are shown in Fig. 5. The results illustrated that the non-focal signals are more irregular than the focal ones. This fact is consistent with previous studies [4], [74], [78]. It should

be noted that the average entropy values over 2 channels for these bivariate EEG signals are reported for the entropy methods.

For each approach, the non-parametric Mann-Whitney U-test was employed to assess the differences between results for the focal and non-focal signals, because the entropy values for all the FuzEn metrics did not follow a normal distribution. The results are presented in Fig. 5. The p-values show that all the methods are similar in terms of discrimination of the focal EEGs from non-focal signals. The Hedges' g effect size [79] was also employed to assess the differences between results for focal vs. non-focal signals. The differences, illustrated

TABLE 2. Sum of the CV values obtained by FuzEn with different fuzzy MFs for forty realizations of MIX process with length 100 and 1,000 sample points.

Membership function $\rightarrow$	Bell-shaped ($n_b = 2$)	Bell-shaped ($n_b = 3$)	Gaussian	Constant-Gaussian	Exponential ($n_e = 3$)	Exponential ($n_e = 4$)
100 samples	1.5973	1.6907	1.6290	1.7082	1.6675	1.6831
1000 samples	0.4177	0.4156	0.4145	0.4109	0.4067	0.4005
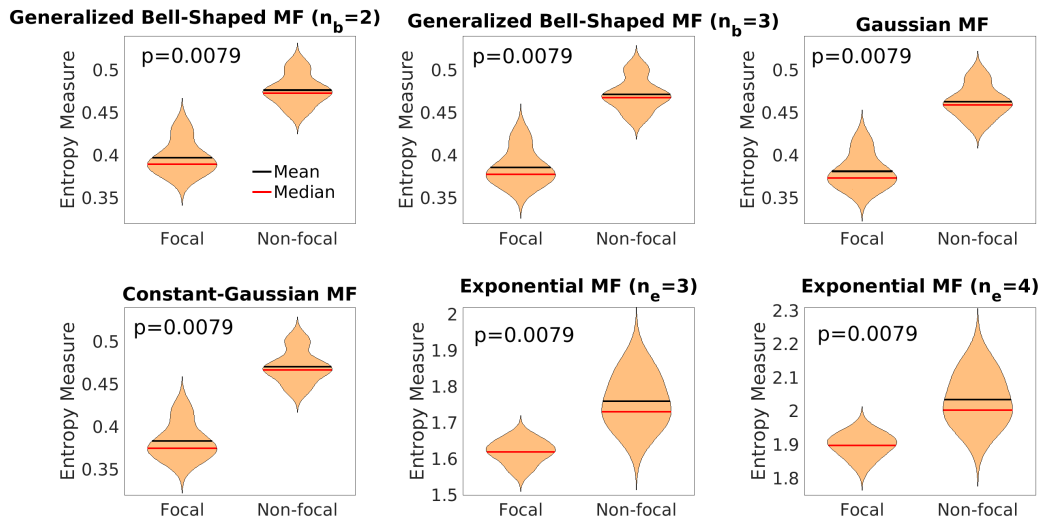
FIGURE 5. Mean and median of results obtained by FuzEn with different fuzzy MFs computed from the focal and non-focal EEG signals. *p* value shown in each panel was from the Mann-Whitney *U*-test for the focal and non-focal EEG signals.

TABLE 3. Differences between results for 1) focal vs. non-focal EEGs; 2) RR interval data for healthy young vs. healthy elderly subjects; and 3) stride interval fluctuations for 3-4 vs. 6-7 years old children (gait maturation) obtained by FuzEn with different fuzzy membership functions based on the Hedges' *g* effect size.

Dataset	Bell-shaped ($n_b = 2$)	Bell-shaped ($n_b = 3$)	Gaussian	Constant-Gaussian	Exponential ($n_e = 3$)	Exponential ($n_e = 4$)
Focal and non-focal EEGs	4.622	4.695	4.696	4.695	2.928	2.726
RR interval data	0.688	0.735	0.679	0.748	0.735	0.751
Gait maturation	0.411	0.390	0.379	0.388	2.434	2.739

in Table 3, show that the best algorithm is FuzEn with Gaussian. Thus, based on these results and those for the MIX process with length 1,000 sample points and the fact that Gaussian function leads to the fastest FuzEn (please see VI), we propose to use FuzEn with Gaussian MF for long signals.

### 2) RR INTERVAL DATA: HEALTHY YOUNG VS. HEALTHY ELDERLY SUBJECTS

In order to compare the performance of FuzEn with different MFs in analyzing short data, only the first 50 sampling points (i.e., 50 normal sinus R-R intervals) of each RR time series were used in this study. Six FuzEn metrics (i.e., FuzEn with bell-shaped MF of order 2, bell-shaped MF of order 3, Gaussian MF, constant-Gaussian MF, exponential MF of order 3, and exponential MF of order 4) were employed. $m = 2$ and $Cr = 0.1$ were set for this application. Results are depicted in Fig. 6. The results illustrate that young subjects' RR interval data are more irregular than those for the elderly people. This finding is in agreement with the fact that aging is associated with loss of irregularity in heart rate control [80].

Results of all the six FuzEn metrics were first tested by the Shapiro-Wilk test to evaluate the normality of the results. The test confirmed the hypothesis of normality with the significance level of 0.05. Student's *t*-test was therefore used to examine their differences between young and old groups. The *p*-values illustrate that FuzEn metrics with all the six MFs show statistically significant between-group differences. FuzEn with constant-Gaussian and exponential MFs of order 4 is able to discriminate the young from elderly subjects slightly better than the other FuzEn metrics.

The differences for the 20 elderly vs. 20 young subjects based on Hedges' *g* effect size are illustrated in Table 3. Although there is no big difference among the results for these six MFs, FuzEn with exponential MF of order 4 led to the highest effect size.

3) GAIT MATURATION DATABASE

The results, depicted in Fig. 7, show that the average entropy values obtained by mean and median values for FuzEn with different membership functions for the elderly children are smaller than those for the young children, in agreement
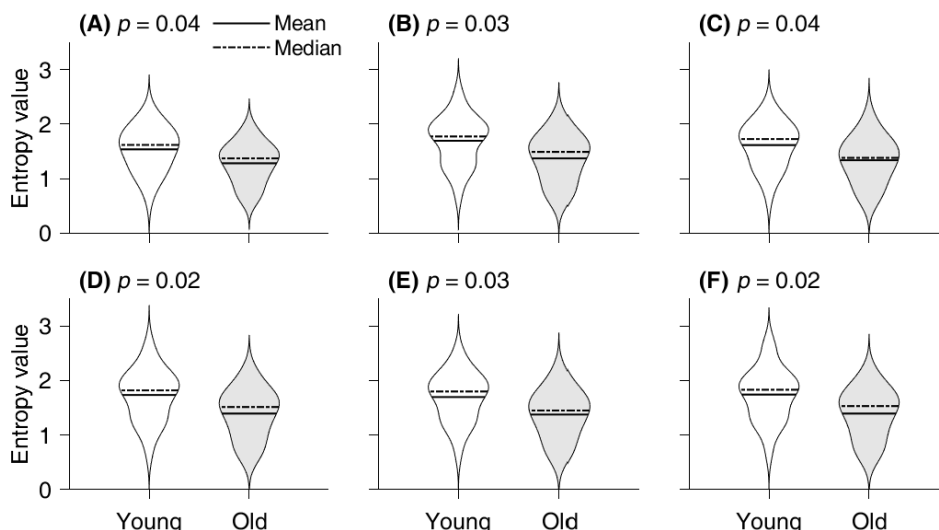
FIGURE 6. Mean and median of results for FuzEn metrics calculated using (A) bell-shaped MF of order 2, (B) bell-shaped MF of order 3, (C) Gaussian MF, (D) constant-Gaussian MF, (E) exponential MF of order 3, and (F) exponential MF of order 4 for the RR interval data in 20 healthy young and 20 healthy elderly subjects. Student's *t*-test *p* value are shown in upper right corner of each panel.

with [77], [81] and the fact that in very young children, immature control of posture and gait leads to unsteady loco-motion [77].

The parameters values for the entropy methods are equal to those used for the above-mentioned real datasets. The differences for the elderly vs. young children based on Mann-Whitney *U*-test, shown in Fig. 7, demonstrate that FuzEn with exponential MF of orders 3 and 4 are only methods that were able to significantly distinguish the elderly vs. young children. The differences for the elderly vs. young children based on Hedges' *g* effect size are illustrated in Table 3. The results show that FuzEn with exponential MF of order 4 outperforms the other methods to discriminate the stride interval time series for 3-4 years old healthy children from those for 6-7 years old subjects.

Overall, FuzEn with exponential MF of order 4 was the best FuzEn-based algorithm for characterization of short white, pink, and brown noises, RR interval time series, and gait maturation data.

VI. COMPUTATIONAL TIME

In order to assess the computational time of FuzEn with different fuzzy MFs, we used white Gaussian noise (WGN) times series with different lengths, logarithmically changing from 300 to 30,000 sample points. The results are illustrated in Table 4. The simulations have been carried out using a PC with Intel (R) Xeon (R) CPU, E5420, 2.5 GHz and 8-GB RAM by MATLAB R2015a. The embedding dimension m and Cr for all the simulations were set as 2 and 0.1, respectively.

The FuzEn methods based on triangular and trapezoidal MFs have one and two conditionally defined expressions, respectively. Therefore, the triangular-based FuzEn is faster.

TABLE 4. computational time of FuzEn with different fuzzy MFs for WGN with different lengths (300, 1,000, 3,000, 10,000, and 30,000 sample points).

Number of samples →	300	1,000	3,000	10,000	30,000
Triangular	0.0019 s	0.0093 s	0.0837 s	0.8997 s	7.4721 s
Trapezoidal	0.0020 s	0.0095 s	0.0920 s	1.1125 s	8.8385 s
Z-shaped	0.0025 s	0.0127 s	0.1296 s	1.3499 s	10.7994 s
Bell-shaped ($n_b = 2$)	0.0042 s	0.0201 s	0.1760 s	1.9314 s	14.7758 s
Bell-shaped ($n_b = 3$)	0.0039 s	0.0198 s	0.1739 s	1.9595 s	15.1232 s
Gaussian	0.0019 s	0.0083 s	0.0604 s	0.5883 s	4.6232 s
Constant-Gaussian	0.0030 s	0.0176 s	0.2440 s	2.5006 s	19.8387 s
Exponential ($n_e = 3$)	0.0040 s	0.0226 s	0.1438 s	1.8340 s	16.8955 s
Exponential ($n_e = 4$)	0.0043 s	0.0227 s	0.1711 s	2.0764 s	16.7386 s

The definitions of FuzEn with Z-shaped and trapezoidal MFs include two conditional expressions. Nevertheless, as the trapezoidal MF is a piecewise linear function, its computational time is lower.

The results show that the fuzzy power for the bell-shaped and exponential MFs does not change the computational time considerably. FuzEn with Gaussian MF is the fastest technique since it does not have any conditionally defined expression or function. It is worth noting that the Gaussian MF is faster than the exponential MF ($n_e = 3$, and 4) because the former has a smaller exponent.

VII. ADVANTAGES AND LIMITATIONS

FuzEn has the advantage, compared to SampEn (and approximate entropy), of not relying on a two-state classifier for judging the similarity or dissimilarity of two vectors (as does the Heaviside function). Therefore, FuzEn, compared
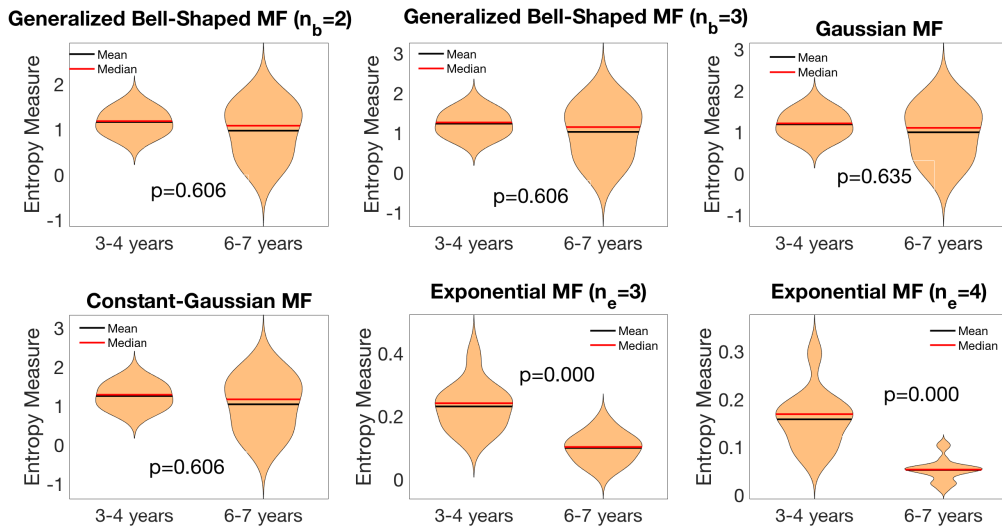
FIGURE 7. Mean and median of results obtained by FuzEn with different fuzzy MFs computed from the stride interval fluctuations for 3-4 vs. 6-7 years old healthy children. *p* value shown in each panel was from the Mann-Whitney *U*-test.

with SampEn and approximate entropy, is less affected by the length of data and similarity degree or threshold r, and shows a better relative consistency [23], [82]. FuzEn also improves the poor statistical stability of approximate entropy and SampEn [23], [82]. Finally, FuzEn with exponential, Gaussian, constant-Gaussian, or generalized bell-shaped MFS, unlike SampEn and approximate entropy, does not lead to undefined values.

One of the limitations that FuzEn possesses is that it does not examine the signal over multiple temporal scales which is however inherent in physiological signals. The multiscale counterpart, namely, the multiscale FuzEn (MFE) [83] may serve as one of the promising solutions. Besides, the refined composite MFE (RCMFE) [22] and inherent FuzEn (InFE) [84] were proposed as well to alleviate the problem of unreliable performance of MFE at larger time scales. The differences between these complexity methods are detailed in [85].

VIII. CONCLUSIONS AND FUTURE DIRECTIONS
In this article, the biomedical applications of the FuzEn metrics were surveyed. We then compared three main FuzEn methods with various fuzzy MFs. Particular attention was given to the importance of an equal center of gravity for different fuzzy MFs. This allowed us to compare FuzEn with different MFs reliably. To evaluate the fuzzy functions, several synthetic and three publicly-available datasets were used.

The present study has the following implications for FuzEn metrics. First, among the three main FuzEn algorithms, FuzEn$^{(Glb)}$ is the only one able to calculate FuzEn with embedding dimension 1 and directly follows the algorithm of very popular SampEn as well. Second, FuzEn with triangular, trapezoidal, and Z-shaped MFs may lead to undefined

entropy values for short time series. Third, FuzEn with bell-shaped ($n_b = 2$), bell-shaped ($n_b = 3$), Gaussian, and constant-Gaussian MFs led to approximately equal Hedges' g effect sizes for long signals (longer than 500 sample points - focal and non-focal EGGs). Additionally, the ability of this FuzEn with Gaussian was similar to FuzEn based on the other MFs for the long synthetic signals (MIX process with length 1,000 sample points). Thus, since the fastest FuzEn method was Gaussian MF, we recommend using FuzEn with Gaussian MF for long signals. Finally, FuzEn based on exponential MF of order 4 was able to distinguish short white, pink, and brown noises, and resulted in more significant differences and higher Hedges' g effect sizes for the short real signals (i.e., RR interval data and stride interval fluctuations). Therefore, FuzEn with exponential MF of order 4 is suggested for short time series (around 50-400 sample points).

There are still two main challenges open to future investigation, namely:

- Although we proposed to use an equal value of the centroid Cr for different fuzzy MFs to reliably compare various FuzEn metrics, we suggest investigating how to choose an optimal Cr (or equivalently, the threshold r) for these approaches.
- The computational time of FuzEn methods is considerably higher than that of dispersion entropy [3] and permutation entropy [86]. Thus, the implementation of FuzEn is needed to be optimized in the future.

Cross-approximate [87] and cross-sample entropy [2], which measure the synchrony (or similarity) of patterns between two times series, have been used in many real-world applications [88]–[93]. Although cross-FuzEn has been developed as a modified form of these approaches [94], there is a need to compare different cross-FuzEn methods based on the local and global characteristics of the embedded vectors of

time series. We also recommend investigating different fuzzy MFs for theses methods. In addition, sample and distribution entropy methods have recently been extended to their two-dimensional cases to quantify the irregularity of textures or images [95], [96]. Due to the advantages of FuzEn over SampEn [23], there is a potential to develop two-dimensional FuzEn with different fuzzy MFs.

ACKNOWLEDGMENT

REFERENCES
[1] C. E. Shannon, "Communication theory of secrecy systems," *Bell Labs Tech. J.*, vol. 28, no. 4, pp. 656–715, Oct. 1949.

[2] J. S. Richman and J. R. Moorman, "Physiological time-series analysis using approximate entropy and sample entropy," *Amer. J. Physiol.-Heart Circulatory Physiol.*, vol. 278, no. 6, pp. H2039–H2049, 2000.

[3] H. Azami and J. Escudero, "Amplitude- and fluctuation-based dispersion entropy," *Entropy*, vol. 20, no. 3, p. 210, Mar. 2018.

[4] M. Rostaghi and H. Azami, "Dispersion entropy: A measure for time-series analysis," *IEEE Signal Process. Lett.*, vol. 23, no. 5, pp. 610–614, May 2016.

[5] J. Cimbálník, A. Hewitt, G. Worrell, and M. Stead, "The CS algorithm: A novel method for high frequency oscillation detection in EEG," *J. Neurosci. Methods*, vol. 293, pp. 6–16, Jan. 2018.

[6] J. Dauwels, F. Vialatte, T. Musha, and A. Cichocki, "A comparative study of synchrony measures for the early diagnosis of Alzheimer's disease based on EEG," *NeuroImage*, vol. 49, no. 1, pp. 668–693, Jan. 2010.

[7] L. Faes, A. Porta, and G. Nollo, "Information decomposition in bivariate systems: Theory and application to cardiorespiratory dynamics," *Entropy*, vol. 17, no. 1, pp. 277–303, 2015.

[8] A. De Luca and S. Termini, "A definition of a nonprobabilistic entropy in the setting of fuzzy sets theory," *Inf. Control*, vol. 20, pp. 301–312, May 1972.

[9] R. R. Yager, "On the entropy of fuzzy measures," *IEEE Trans. Fuzzy Syst.*, vol. 8, no. 4, pp. 453–461, Aug. 2000.

[10] W. Sander, "On measures of fuzziness," *Fuzzy Sets Syst.*, vol. 29, no. 1, pp. 49–55, 1989.

[11] S. Al-Sharhan, F. Karray, W. Gueaieb, and O. Basir, "Fuzzy entropy: A brief survey," in *Proc. 10th IEEE Int. Conf. Fuzzy Syst.*, vol. 3, Dec. 2001, pp. 1135–1139.

[12] R. Ferenets, T. Lipping, A. Anier, V. Jantti, S. Melto, and S. Hovilehto, "Comparison of entropy and complexity measures for the assessment of depth of sedation," *IEEE Trans. Biomed. Eng.*, vol. 53, no. 6, pp. 1067–1077, Jun. 2006.

[13] S. Chaibi, Z. Sakka, T. Lajnef, M. Samet, and A. Kachouri, "Automated detection and classification of high frequency oscillations (HFOs) in human intracereberal EEG," *Biomed. Signal Process. Control*, vol. 8, no. 6, pp. 927–934, 2013.

[14] M. Navarrete, J. Pyrzowski, J. Corlier, M. Valderrama, and M. Quyen, "Automated detection of high-frequency oscillations in electrophysiological signals: Methodological advances," *J. Physiol.-Paris*, vol. 110, pp. 316–326, Nov. 2018.

[15] S. Sanei and J. A. Chambers, *EEG Signal Processing*. Hoboken, NJ, USA: Wiley, 2007, pp. 1–20.

[16] X. Hu, J. Jiang, D. Cao, and B. Egardt, "Battery health prognosis for electric vehicles using sample entropy and sparse Bayesian predictive modeling," *IEEE Trans. Ind. Electron.*, vol. 63, no. 4, pp. 2645–2656, Apr. 2016.

[17] Z.-H. Zhao and S.-P. Yang, "Sample entropy-based roller bearing fault diagnosis method," *J. Vib. Shock*, vol. 31, no. 6, pp. 136–140, 2012.

[18] M. Han and J. Pan, "A fault diagnosis method combined with LMD, sample entropy and energy ratio for roller bearings," *Measurement*, vol. 76, pp. 7–19, Dec. 2015.

[19] X. Jie, R. Cao, and L. Li, "Emotion recognition based on the sample entropy of EEG," *Biomed. Mater. Eng.*, vol. 24, no. 1, pp. 1185–1192, 2014.

[20] L. A. Zadeh, "Fuzzy sets," *Inf. Control*, vol. 8, no. 3, pp. 338–353, Jun. 1965.

[21] P. Li, C. Liu, K. Li, D. Zheng, C. Liu, and Y. Hou, "Assessing the complexity of short-term heartbeat interval series by distribution entropy," *Med. Biol. Eng. Comput.*, vol. 53, no. 1, pp. 77–87, 2015.

[22] H. Azami, A. Fernández, and J. Escudero, "Refined multiscale fuzzy entropy based on standard deviation for biomedical signal analysis," *Med. Biol. Eng. Comput.*, vol. 55, no. 11, pp. 2037–2052, 2017.

[23] W. Chen, Z. Wang, H. Xie, and W. Yu, "Characterization of surface EMG signal based on fuzzy entropy," *IEEE Trans. Neural Syst. Rehabil. Eng.*, vol. 15, no. 2, pp. 266–272, Jun. 2007.

[24] W. Chen, J. Zhuang, W. Yu, and Z. Wang, "Measuring complexity using FuzzyEn, ApEn, and SampEn," *Med. Eng. Phys.*, vol. 31, no. 1, pp. 61–68, 2009.

[25] G. Wang and J. Wang, "New approach of financial volatility duration dynamics by stochastic finite-range interacting voter system," *Chaos, Interdiscipl. J. Nonlinear Sci.*, vol. 27, no. 1, 2017, Art. no. 013117.

[26] W. Deng, R. Yao, M. Sun, H. Zhao, Y. Luo, and C. Dong, "Study on a novel fault diagnosis method based on integrating EMD, fuzzy entropy, improved PSO and SVM," *J. Vibroeng.*, vol. 19, no. 4, pp. 2562–2577, 2017.

[27] H.-B. Xie, B. Sivakumar, T. W. Boonstra, and K. Mengersen, "Fuzzy entropy and its application for enhanced subspace filtering," *IEEE Trans. Fuzzy Syst.*, vol. 26, no. 4, pp. 1970–1982, Aug. 2018. doi: 10.1109/TFUZZ.2017.2756829.

[28] E. Reinertsen, M. Osipov, C. Liu, J. M. Kane, G. Petrides, and G. D. Clifford, "Continuous assessment of schizophrenia using heart rate and accelerometer data," *Physiolog. Meas.*, vol. 38, no. 7, p. 1456, 2017.

[29] H.-B. Xie, W.-T. Chen, W.-X. He, and H. Liu, "Complexity analysis of the biomedical signal using fuzzy entropy measurement," *Appl. Soft Comput.*, vol. 11, no. 2, pp. 2871–2879, 2011.

[30] C. Liu, K. Li, L. Zhao, F. Liu, D. Zheng, C. Liu, and S. Liu, "Analysis of heart rate variability using fuzzy measure entropy," *Comput. Biol. Med.*, vol. 43, no. 2, pp. 100–108, 2013.

[31] B. Shi, Y. Zhang, C. Yuan, S. Wang, and P. Li, "Entropy analysis of short-term heartbeat interval time series during regular walking," *Entropy*, vol. 19, no. 10, p. 568, 2017.

[32] M. U. Ahmed, T. Chanwimalueang, S. Thayyil, and D. P. Mandic, "A multivariate multiscale fuzzy entropy algorithm with application to uterine EMG complexity analysis," *Entropy*, vol. 19, no. 1, p. 2, 2016.

[33] P. Li, L. Ji, C. Yan, K. Li, C. Liu, and C. Liu, "Coupling between short-term heart rate and diastolic period is reduced in heart failure patients as indicated by multivariate entropy analysis," in *Proc. Comput. Cardiol. Conf. (CinC)*, Sep. 2014, pp. 97–100.

[34] J. Hu, "An approach to EEG-based gender recognition using entropy measurement methods," *Knowl.-Based Syst.*, vol. 140, pp. 134–141, Jan. 2018.

[35] Z. Mu, J. Hu, J. Min, and J. Yin, "Comparison of different entropies as features for person authentication based on EEG signals," *IET Biometrics*, vol. 6, no. 6, pp. 409–417, Nov. 2017.

[36] Z. Mu, J. Hu, and J. Min, "EEG-based person authentication using a fuzzy entropy-related approach with two electrodes," *Entropy*, vol. 18, no. 12, p. 432, 2016.

[37] M. N. Tibdewal, H. R. Dey, M. Mahadevappa, A. Ray, and M. Malokar, "Multiple entropies performance measure for detection and localization of multi-channel epileptic EEG," *Biomed. Signal Process. Control*, vol. 38, pp. 158–167, Sep. 2017.

[38] J. Xiang, C. Li, H. Li, R. Cao, B. Wang, X. Han, and J. Chen, "The detection of epileptic seizure signals based on fuzzy entropy," *J. Neurosci. Methods*, vol. 243, pp. 18–25, Mar. 2015.

[39] Y. Cao, L. Cai, J. Wang, R. Wang, H. Yu, Y. Cao, and J. Liu, "Characterization of complexity in the electroencephalograph activity of Alzheimer's disease based on fuzzy entropy," *Chaos*, vol. 25, no. 8, 2015, Art. no. 083116.

[40] S. Simons, P. Espino, and D. Abásolo, "Fuzzy entropy analysis of the electroencephalogram in patients with Alzheimer's disease: Is the method superior to sample entropy?" *Entropy*, vol. 20, no. 1, p. 21, 2018.

[41] S.-Y. Lin, C.-W. Jao, P.-S. Wang, and Y.-T. Wu, "Analysis of electroencephalography alteration during sustained cycling exercise using power spectrum and fuzzy entropy," *Int. J. Fuzzy Syst.*, vol. 19, no. 2, pp. 580–590, 2017.

[42] H. Liu, X. Hongbo, H. Weixing, and W. Zhizhong, "Characterization and classification of EEG sleep stage based on fuzzy entropy," *J. Data Acquisition Process.*, vol. 25, no. 14, pp. 484–489, 2010.

[43] J. Hu and P. Wang, "Noise robustness analysis of performance for EEG-based driver fatigue detection using different entropy feature sets," *Entropy*, vol. 19, no. 8, p. 385, 2017.

[44] J. Hu, "Comparison of different features and classifiers for driver fatigue detection based on a single EEG channel," *Comput. Math. Methods Med.*, vol. 2017, Jan. 2017, Art. no. 5109530.

[45] J. Monge, C. Gómez, J. Poza, A. Fernández, J. Quintero, and R. Hornero, "MEG analysis of neural dynamics in attention-deficit/hyperactivity disorder with fuzzy entropy," *Med. Eng. Phys.*, vol. 37, no. 4, pp. 416–423, 2015.

[46] X. Zhu, X. Zhang, X. Tang, X. Gao, and X. Chen, "Re-evaluating electromyogram–force relation in healthy biceps brachii muscles using complexity measures," *Entropy*, vol. 19, no. 11, p. 624, 2017.

[47] W. Sun, J. Liang, Y. Yang, Y. Wu, T. Yan, and R. Song, "Investigating aging-related changes in the coordination of agonist and antagonist muscles using fuzzy entropy and mutual information," *Entropy*, vol. 18, no. 6, p. 229, 2016.

[48] U. R. Acharya, Y. Hagiwara, J. E. W. Koh, S. L. Oh, J. H. Tan, M. Adam, and R. S. Tan, "Entropies for automated detection of coronary artery disease using ECG signals: A review," *Biocybern. Biomed. Eng.*, vol. 38, no. 2, pp. 373–384, 2018.

[49] B. Chicote, U. Irusta, R. Alcaraz, J. J. Rieta, E. Aramendi, I. Isasi, D. Alonso, and K. Ibarguren, "Application of entropy-based features to predict defibrillation outcome in cardiac arrest," *Entropy*, vol. 18, no. 9, p. 313, 2016.

[50] Y. Zhang and L. Ni, "Speech activity detection based on fuzzy entropy and improved relevance vector machine," *J. Huazhong Univ. Sci. Technol. (Natural Sci. Ed.)*, vol. 45, pp. 15–19, Aug. 2017.

[51] R. J. Elton, P. Vasuki, and J. Mohanalin, "Voice activity detection using fuzzy entropy and support vector machine," *Entropy*, vol. 18, no. 8, p. 298, 2016.

[52] L. Ji, P. Li, K. Li, X. Wang, and C. Liu, "Analysis of short-term heart rate and diastolic period variability using a refined fuzzy entropy method," *Biomed. Eng. Online*, vol. 14, no. 1, p. 64, Jul. 2015.

[53] K. Zhu, X. Jiang, L. Chen, and H. Li, "Performance degradation assessment of rolling element bearings using improved fuzzy entropy," *Meas. Sci. Rev.*, vol. 17, no. 5, pp. 219–225, 2017.

[54] M. Costa, A. L. Goldberger, and C.-K. Peng, "Multiscale entropy analysis of biological signals," *Phys. Rev. E, Stat. Phys. Plasmas Fluids Relat. Interdiscip. Top.*, vol. 71, no. 2, 2005, Art. no. 021906.

[55] D. E. Lake, J. S. Richman, M. P. Griffin, and J. R. Moorman, "Sample entropy analysis of neonatal heart rate variability," *Amer. J. Physiol.-Regulatory, Integrative Comparative Physiol.*, vol. 283, no. 3, pp. R789–R797, 2002.

[56] S. Lu, X. Chen, J. K. Kanters, I. C. Solomon, and K. H. Chon, "Automatic selection of the threshold value *r* for approximate entropy," *IEEE Trans. Biomed. Eng.*, vol. 55, no. 8, pp. 1966–1972, Aug. 2008.

[57] W. Van Leekwijck and E. E. Kerre, "Defuzzification: Criteria and classification," *Fuzzy Sets Syst.*, vol. 108, no. 2, pp. 159–178, 1999.

[58] A. Escobet, A. Nebot, and F. E. Cellier, "Fault diagnosis system based on fuzzy logic: Application to a valve actuator benchmark," *J. Intell. Fuzzy Syst.*, vol. 22, no. 4, pp. 155–171, 2011.

[59] T. J. Ross, *Fuzzy Logic With Engineering Applications*. Hoboken, NJ, USA: Wiley, 2009.

[60] C. C. Lee, "Fuzzy logic in control systems: Fuzzy logic controller. II," *IEEE Trans. Syst., Man, Cybern.*, vol. 20, no. 2, pp. 419–435, Mar./Apr. 1990.

[61] J. Zhao and B. K. Bose, "Evaluation of membership functions for fuzzy logic controlled induction motor drive," in *Proc. IEEE 28th Annu. Conf. Ind. Electron. Soc.*, vol. 1, Nov. 2002, pp. 229–234.

[62] W. Pedrycz, "Why triangular membership functions?" *Fuzzy Sets Syst.*, vol. 64, no. 1, pp. 21–30, 1994.

[63] W. Duch, "Uncertainty of data, fuzzy membership functions, and multilayer perceptrons," *IEEE Trans. Neural Netw.*, vol. 16, no. 1, pp. 10–23, Jan. 2005.

[64] O. Castillo and P. Melin, *Soft Computing for Control of Non-Linear Dynamical Systems*, vol. 63. Springer, 2012.

[65] A. Asemi, S. S. B. Salim, S. R. Shahamiri, A. Asemi, and N. Houshangi, "Adaptive neuro-fuzzy inference system for evaluating dysarthric automatic speech recognition (ASR) systems: A case study on MVML-based ASR," *Soft Comput.*, vol. 23, no. 10, pp. 3529–3544, 2019. doi: 10.1007/s00500-018-3013-4.

[66] A. Salimi, J. Rostami, C. Moormann, and A. Delisio, "Application of non-linear regression analysis and artificial intelligence algorithms for performance prediction of hard rock TBMs," *Tunnelling Underground Space Technol.*, vol. 58, pp. 236–246, Sep. 2016.

[67] G. Klir and B. Yuan, *Fuzzy Sets Fuzzy Logic*, vol. 4. Upper Saddle River, NJ, USA: Prentice-Hall, 1995.

[68] L. Cohen, "The history of noise [on the 100th anniversary of its birth]," *IEEE Signal Process. Mag.*, vol. 22, no. 6, pp. 20–45, Nov. 2005.

[69] E. Sejdić and L. A. Lipsitz, "Necessity of noise in physiology and medicine," *Comput. Methods Programs Biomed.*, vol. 111, no. 2, pp. 459–470, 2013.

[70] M. S. Keshner, "1/f noise," *Proc. IEEE*, vol. 70, no. 3, pp. 212–218, Mar. 1982.

[71] S. M. Pincus, "Approximate entropy as a measure of system complexity," *Proc. Nat. Acad. Sci. USA*, vol. 88, no. 6, pp. 2297–2301, 1991.

[72] M. Ferrario, M. G. Signorini, G. Magenes, and S. Cerutti, "Comparison of entropy-based regularity estimators: Application to the fetal heart rate signal for the identification of fetal distress," *IEEE Trans. Biomed. Eng.*, vol. 53, no. 1, pp. 119–125, Jan. 2006.

[73] S. M. Pincus and A. L. Goldberger, "Physiological time-series analysis: What does regularity quantify?" *Amer. J. Physiol.-Heart Circulatory Physiol.*, vol. 266, no. 4, pp. H1643–H1656, 1994.

[74] R. G. Andrzejak, K. Schindler, and C. Rummel, "Nonrandomness, nonlinear dependence, and nonstationarity of electroencephalographic recordings from epilepsy patients," *Phys. Rev. E, Stat. Phys. Plasmas Fluids Relat. Interdisc. Top.*, vol. 86, no. 4, 2012, Art. no. 046206.

[75] A. L. Goldberger, L. A. Amaral, L. Glass, J. M. Hausdorff, P. C. Ivanov, R. G. Mark, J. E. Mietus, G. B. Moody, C.-K. Peng, and H. E. Stanley, "PhysioBank, PhysioToolkit, and PhysioNet: Components of a new research resource for complex physiologic signals," *Circulation*, vol. 101, no. 23, pp. e215–e220, 2000.

[76] N. Iyengar, C. K. Peng, R. Morin, A. L. Goldberger, and L. A. Lipsitz, "Age-related alterations in the fractal scaling of cardiac interbeat interval dynamics," *Amer. J. Physiol.-Regulatory, Integrative Comparative Physiol.*, vol. 271, no. 4, pp. R1078–R1084, 1996.

[77] J. M. Hausdorff, L. Zemany, C. K. Peng, and A. L. Goldberger, "Maturation of gait dynamics: Stride-to-stride variability and its temporal organization in children," *J. Appl. Physiol.*, vol. 86, no. 3, pp. 1040–1047, 1999.

[78] R. Sharma, R. Pachori, and U. Acharya, "Application of entropy measures on intrinsic mode functions for the automated identification of focal electroencephalogram signals," *Entropy*, vol. 17, no. 2, pp. 669–691, 2015.

[79] R. Rosenthal, H. Cooper, and L. Hedges, "Parametric measures of effect size," in *The Handbook of Research Synthesis*, vol. 621. 1994, pp. 231–244.

[80] A. L. Goldberger, C. K. Peng, and L. A. Lipsitz, "What is physiologic complexity and how does it change with aging and disease?" *Neurobiol. Aging*, vol. 23, no. 1, pp. 23–26, Jan./Feb. 2002.

[81] M. C. Bisi and R. Stagni, "Complexity of human gait pattern at different ages assessed using multiscale entropy: From development to decline," *Gait Posture*, vol. 47, pp. 37–42, Jun. 2016.

[82] P. Li, C. Liu, X. Wang, B. Li, W. Che, and C. Liu, "Cross-sample entropy and cross-fuzzy entropy for testing pattern synchrony: How results vary with different threshold value *r*," in *World Congress on Medical Physics and Biomedical Engineering*. Beijing, China: Springer, May 2012, pp. 485–488.

[83] J. Zheng, J. Cheng, Y. Yang, and S. Luo, "A rolling bearing fault diagnosis method based on multi-scale fuzzy entropy and variable predictive model-based class discrimination," *Mechanism Mach. Theory*, vol. 78, no. 16, pp. 187–200, 2014.

[84] Z. Cao and C.-T. Lin, "Inherent fuzzy entropy for the improvement of EEG complexity evaluation," *IEEE Trans. Fuzzy Syst.*, vol. 26, no. 2, pp. 1032–1035, Apr. 2018. doi: 10.1109/TFUZZ.2017.2666789.

[85] H. Azami and J. Escudero, "Coarse-graining approaches in univariate multiscale sample and dispersion entropy," *Entropy*, vol. 20, no. 2, p. 138, Feb. 2018.

[86] C. Bandt and B. Pompe, "Permutation entropy: A natural complexity measure for time series," *Phys. Rev. Lett.*, vol. 88, no. 17, 2002, Art. no. 174102.

[87] S. Pincus and B. H. Singer, "Randomness and degrees of irregularity," *Proc. Nat. Acad. Sci. USA*, vol. 93, no. 5, pp. 2083–2088, 1996.

[88] W. Shi and P. Shang, "Cross-sample entropy statistic as a measure of synchronism and cross-correlation of stock markets," *Nonlinear Dyn.*, vol. 71, no. 3, pp. 539–554, 2013.

[89] L.-Z. Liu, X.-Y. Qian, and H.-Y. Lu, "Cross-sample entropy of foreign exchange time series," *Phys. A, Stat. Mech. Appl.*, vol. 389, no. 21, pp. 4785–4792, 2010.

[90] T. Zhang, Z. Yang, and J. H. Coote, "Cross-sample entropy statistic as a measure of complexity and regularity of renal sympathetic nerve activity in the rat," *Exp. Physiol.*, vol. 92, no. 4, pp. 659–669, 2007.

[91] A. G. Hudetz, J. D. Wood, and J. P. Kampine, "Cholinergic reversal of isoflurane anesthesia in rats as measured by cross-approximate entropy of the electroencephalogram," *Anesthesiol., J. Amer. Soc. Anesthesiolog.*, vol. 99, no. 5, pp. 1125–1131, 2003.

[92] A. G. Hudetz, "Effect of volatile anesthetics on interhemispheric EEG cross-approximate entropy in the rat," *Brain Res.*, vol. 954, no. 1, pp. 123–131, 2002.

[93] P. Li, C. Liu, X. Wang, L. Li, L. Yang, Y. Chen, and C. Liu, "Testing pattern synchronization in coupled systems through different entropy-based measures," *Med. Biol. Eng. Comput.*, vol. 51, no. 5, pp. 581–591, 2013.

[94] H.-B. Xie, Y.-P. Zheng, J.-Y. Guo, and X. Chen, "Cross-fuzzy entropy: A new method to test pattern synchrony of bivariate time series," *Inf. Sci.*, vol. 180, no. 9, pp. 1715–1724, 2010.

[95] H. Azami, J. Escudero, and A. Humeau-Heurtier, "Bidimensional distribution entropy to analyze the irregularity of small-sized textures," *IEEE Signal Process. Lett.*, vol. 24, no. 9, pp. 1338–1342, Sep. 2017.

[96] L. E. V. Silva, A. C. S. Filho, V. P. S. Fazan, J. C. Felipe, and L. O. M. Junior, "Two-dimensional sample entropy: Assessing image texture through irregularity," *Biomed. Phys. Eng. Express*, vol. 2, no. 4, 2016, Art. no. 045002.

STEVEN E. ARNOLD received the M.D. degree from Boston University, USA. He held residency training in psychiatry at the New York State Psychiatric Institute/Columbia Presbyterian Medical Center, New York, and residency training in neurology at the University of Iowa Hospitals and Clinics, Iowa. He also held fellowship training in Behavioral Neurology/Cognitive Neuroscience and was a Postdoctoral Associate in Neuroanatomy, Iowa. He is board certified in neurology and psychiatry. He joined the Faculty at the University of Pennsylvania, where he was a Professor of psychiatry and neurology until his move to Massachusetts General Hospital (MGH) in 2015.

At MGH, he is currently leading the Interdisciplinary Brain Center, a new collaboration of the Departments of Neurology, Psychiatry, and the Martinos Center for Neuroimaging. Its mission is to facilitate the discovery, development, and implementation of promising therapeutics and associated diagnostics for individuals with complex brain disorders that affect cognition, behavior, and emotion. Major disease interests of the Interdisciplinary Brain Center are Alzheimer's disease and related disorders.

HAMED AZAMI received the Ph.D. degree in biomedical signal processing from the Institute for Digital Communication, The University of Edinburgh, U.K., in 2018. He is currently a Postdoctoral Research Fellow in biomedical signal processing and machine learning with Massachusetts General Hospital and Harvard University, USA. His main research interests include biomedical signal processing, nonlinear analysis, and machine learning.

He served as a Technical Program Committee Member of the IEEE Machine Learning for Signal Processing and the IEEE Conference on Digital Signal Processing. He received the Nightingale Award for the best paper published, in 2017, in medical and biological engineering and computing. He serves as an Associate Editor of IEEE Access. He also served as a Guest Editor for the *Journal of Complexity*.

PENG LI (M'15) was born in Weishan, Shandong, China, in 1988. He received the B.S. and Ph.D. degrees in biomedical engineering from Shandong University, Jinan, China, in 2009 and 2014, respectively.

He held multiple disciplinary postdoctoral trainings, first at Shandong University, from 2014 to 2015, and then at the Harvard Medical School, from 2016 to 2018. He is currently appointed as an Instructor in medicine with the Division of Sleep Medicine, Harvard Medical School, Boston, MA, USA, and an Associate Physiologist with the Division of Sleep and Circadian Disorders, Brigham & Women's Hospital, Boston. His research interests include understanding the nonlinear dynamics in cardiovascular system, brain activity, and motor activity. In particular, he is recently interested in the prediction of Alzheimer's dementia and cardiovascular diseases noninvasively and the underlying neuro-pathological mechanisms.

Dr. Li is a member of the Society for Neuroscience, the Sleep Research Society, the American Academy of Sleep Medicine, the China Biomedical Engineering Society, and the Beijing Society for Cognitive Neuroscience. He was a recipient of the Trainee Professional Development Award from the Society for Neuroscience, in 2018, and the Second Prize of the Science and Technology Award in invention in Shandong, China, in 2016.

JAVIER ESCUDERO (S'07–M'10) received the M.Eng. and Ph.D. degrees in telecommunications engineering from the University of Valladolid, Spain, in 2005 and 2010, respectively. Afterwards, he held a Postdoctoral position at Plymouth University, U.K., until 2013.

He is currently a tenured academic with the School of Engineering, The University of Edinburgh, U.K., where he leads a Research Group in biomedical signal processing. He is the author of over 55 scientific journal articles. His research interests include non-linear analysis, network theory, and multiway decompositions.

Dr. Escudero was elected member of the Young Academy of Scotland, in 2016. He received the Third Prize of the EMBS Student Paper Competition, in 2007, and the Award to the best Ph.D. thesis in healthcare technologies by the Spanish Organization of Telecommunications Engineers, in 2010. He has also received the Nightingale Award for the best paper published, in 2017, in medical and biological engineering and computing. He has served as the President of the Society of Spanish Researchers in the United Kingdom (SRUK) and the Network of Spanish Researchers Abroad (RAICEX), from 2018 to 2019.

ANNE HUMEAU-HEURTIER received the Ph.D. degree in biomedical engineering in France. She is currently a Full Professor of engineering with the University of Angers, France. She is the author/coauthor of more than 80 papers in peer-reviewed journals and has participated in the organization of several conferences and workshops. Her research interests include signal and image processing, mainly multiscale and entropy-based analyses, and data-driven methods. Her main applications are related to the biomedical field. She is a member of the IEEE-EMBS Technical Committee on Cardiopulmonary Systems. She is also a member of the Editorial Board of Entropy. She was the Guest Editor of the special issues in journals, such as the IEEE Transactions on Biomedical Circuits and Systems, *Entropy, Complexity, and Computational and Mathematical Methods in Medicine*. She is also an Associate Editor of the Engineering Medicine and Biological Society Conference.

● ● ●